Adenosine Activates AMPK to Phosphorylate Bcl-X$_L$ Responsible for Mitochondrial Damage and DIABLO Release in HuH-7 Cells

Donqin Yang[1,3], Takahiro Yaguchi[1], Takashi Nakano[2] and Tomoyuki Nishizaki[1]

[1]Division of Bioinformation, Department of Physiology, Hyogo College of Medicine, Nishinomiya [2]Department of Thoracic Oncology, Hyogo College of Medicine, Nishinomiya [3]Laboratory of Molecular Cell Biology, Institute of Biochemistry and Cell Biology, Shanghai Institutes for Biological Sciences, Chinese Academy of Sciences, Shanghai

Abstract
Background/Aims: Accumulating evidence has pointed to AMP-activated protein kinase (AMPK) as an inducer of apoptosis in a variety of cancer cells. The present study aimed at understanding AMPK signals for adenosine-induced HuH-7 cell apoptosis. Methods: Cell viability, AMPK activity, mitochondrial membrane potentials, phosphorylation of Bcl-X$_L$, *in situ* DIABLO mobilizations, and caspase-3 activity were monitored in HuH-7 cells. Plasmid DNAs for DIABLO-GFP, mutant Bcl-X$_L$, dominant negative mutant AMPKα2 and the siRNAs to silence the AMPKα1 or AMPKα2 targeted gene were constructed and transfected. Results: Adenosine or the AMPK activator AICAR induced apoptosis in HuH-7 cells, and no synergistic effect was obtained with co-treatment. Adenosine activated AMPK, to phosphorylate Bcl-X$_L$. Adenosine or AICAR disrupted mitochondrial membrane potentials, and the effect was inhibited by knocking-down AMPKα1 and/or AMPKα2, expressing dominant negative mutant AMPKα2 or mutant Bcl-X$_L$ lacking Ser/Thr phosphorylation sites. AICAR stimulated DIABLO release from the mitochondria, and the release was suppressed by expressing the mutant Bcl-X$_L$. AICAR activated caspase-3, which was also inhibited by expressing the mutant Bcl-X$_L$. Conclusion: Adenosine activates AMPK, to disrupt mitochondrial membrane potentials through Bcl-X$_L$ phosphorylation, allowing DIABLO release from the mitochondria, as a factor for caspase-3 activation to induce HuH-7 cell apoptosis.

Copyright © 2011 S. Karger AG, Basel

Introduction

Extracellular adenosine induces apoptosis in a variety of cancer cells via an intrinsic pathway relevant to adenosine uptake into cells and/or an extrinsic pathway relevant to adenosine receptors such as A_1, A_{2a}, A_{2b}, and A_3 receptors. In our earlier study, adenosine induced apoptosis in HuH-7 cells, a Fas-deficient human hepatoma cell line [1]. Adenosine-induced HuH-7 cell apoptosis was inhibited by dipyridamole, an adenosine transporter inhibitor, or 5'-amino-5'-deoxyadenosine (ADA), an inhibitor of adenosine kinase to convert from adenosine

Prof. Tomoyuki Nishizaki
Division of Bioinformation, Department of Physiology, Hyogo College of Medicine,
1-1 Mukogawa-cho, Nishinomiya 663-8501 (Japan)
Tel. +81-798-45-6397, Fax +81-798-45-6649
E-Mail tomoyuki@hyo-med.ac.jp

to AMP, but the adenosine action was not affected by inhibitors for A_1, A_{2a}, A_{2b}, and A_3 adenosine receptors [1], suggesting mediation of an intrinsic pathway. Adenosine activated caspase-3 and -8, without caspase-9 activation, in HuH-7 cells, and the caspase-8 activation was prevented by expressing c-Fas-associated death domain protein (FADD)-like interleukin-1β-converting enzyme inhibitory protein (c-FLIP) short [1]. Adenosine reduced expression of the c-FLIP mRNA and protein [1]. It is indicated from these results that intracellularly transported adenosine is converted to AMP, which produces a signal to downregulate c-FLIP expression, thereby neutralizing caspase-8 inhibition due to c-FLIP, resulting in the activation of caspase-8 and the effector caspase-3. This accounts for a pathway underlying adenosine-induced HuH-7 cell apoptosis.

Extracellular adenosine, on the other hand, disrupted mitochondrial membrane potentials in HuH-7 cells, and the effect was inhibited by the adenosine transporter inhibitor dipyridamole or by overexpressing Bcl-X_L [2]. Adenosine reduced expression of mRNAs and proteins for Bcl-X_L and inhibitor of apoptosis protein 2 (IAP2), to directly inhibit caspase-3, but adenosine otherwise increased expression of mRNA and protein for DIABLO, an inhibitor of IAPs [2]. Those adenosine effects were attenuated by dipyridamole [2]. Adenosine-induced caspase-3 activation was inhibited by overexpressing Bcl-X_L or IAP2 [2]. Consequently, intracellularly transported adenosine could activate caspase-3, regardless of caspase-9 activation, by neutralizing caspase-3 inhibition due to IAP as a result of decreased IAP2 expression and reduced IAP activity in response to increased DIABLO expression and DIABLO release from damaged mitochondria, in addition to caspse-8 activation. This provides an additional pathway underlying adenosine-induced HuH-7 cell apoptosis. What signal events underlie downstream intracellularly transported adenosine followed by AMP conversion, however, remains an open question. We have found that intracellularly transported adenosine through adenosine transporters induces apoptosis in GT3-TKB human lung cancer cells by activating AMP-activated protein kinase (AMPK) [3]. Then, we thought that AMPK plays a role in adenosine-induced HuH-7 cell apoptosis as well.

We show here that adenosine activates AMPK to phosphorylate Bcl-X_L, thereby perturbing mitochondrial membrane potentials, which triggers DIABLO release from the mitochondria, resulting in caspase-3 activation, independently of caspase-9 activation, to induce HuH-7 cell apoptosis.

Materials and Methods

Materials

AICAR was obtained from Toronto Research Chemicals (North York, Canada). Dipyridamole was from ICN Biomedicals (Aurora, USA). A DePsiper™ kit was from Trevigen (Gaithersburg, USA). An anti-AMPKα1 antibody and an anti-AMPKα2 antibody were from Bethyl Laboratories (San Diego, USA). An anti-phospho-AMPK Thr172 antibody was from Cell Signaling Technology (Beverly, USA). The AMPKα1 siRNA, the AMPKα2 siRNA, an anti-Bcl-X_L antibody, and an anti-DIABLO antibody were from Santa Cruz Biotechnology (Santa Cruz, USA). An anti-phosphoserine/threonine antibody and an anti-prohibitin antibody were from Abcam (Cambridge, USA). An anti-DAPI, MitoTracker Red 580, and a goat anti-rabbit IgG antibody were from Molecular Probes (Eugene, USA). An anti-rabbit IgG antibody was from MP Biomedicals Inc. (Ohio, USA). An anti-mouse IgG antibody was from ICN Pharmaceuticals, Inc. (New York, USA). A protein G agarose and an ECL Plus Western blotting detection reagent were from GE Healthcare Bio-Sciences (Piscataway, USA). A lipofectamine reagent was from Invitrogen Corporation (Carlsbad, USA). A caspase fluorometric assay kit was from BioVision Research Products (Mountain View, USA).

Cell culture

HuH-7 cells were obtained from RIKEN cell bank (Ibaraki, Japan). Cells were cultured in Dulbecco's Modified Eagles Medium supplemented with 10% (v/v) heat-inactivated fetal bovine serum, penicillin (final concentration, 100 U/ml), and streptomycin (final concentration, 0.1 mg/ml), in a humidified atmosphere of 5% CO_2 and 95% air at 37°C.

3-(4,5-Dimethyl-2-thiazolyl)-2,5-diphenyl-2H-tetrazolium bromide (MTT) assay

Cell viability was evaluated by a dye staining method using MTT as previously described [1]. MTT-reactive cells were quantified at an absorbance of 570 nm using a micro-plate reader (SPECTRAmax PLUS384, Molecular Devices, Sunnyvale, USA), and percentage of independent basal levels (MTT intensities of cells untreated with any drug) was calculated.

Plasmid construction and transfection

DIABLO-GFP-pcDNA6/V5 was cloned in the Kpn-1/EcoRV site with C-terminal His tag. DNAs for mutant Bcl-X_L with replacement of Thr47, Ser56, Ser62, and Thr115 by Ala and dominant negative mutant AMPKα2 with replacement Asp157 by Ala (D157A) were cloned in the EcoR I site with pcDNA6/V5. The plasmid DNA for DIABLO-GFP, dominant negative mutant AMPKα2 (D157A) or mutant Bcl-X_L lacking Ser/Thr phosphorylation sites was transfected into cells using an electroporation system (Optimizor500, BTX, San Diego, USA). The small interfering RNA (siRNA) to silence the AMPKα1 (AMPKα1 siRNA) or AMPKα2 targeted gene (AMPKα2 siRNA) was transfected into HuH-7 cells with a lipofectamine reagent. Cells were used for experiments 48 h later after transfection.

Assay of mitochondrial membrane potentials
HuH-7 cells were incubated in a DePsipher™ solution at 37°C for 20 min, and the fluorescent signals were observed with a fluorescent photomicroscope (ECLIPSE TE300, NIKON Co., Kawasaki, Japan) equipped with an epifluorescence device using a fluorescein long-pass filter (fluorescein and rhodamine) at an absorbance of 590 nm for red aggregations and at an absorbance of 530 nm for green aggregations.

Immunocytochemistry
HuH-7 cells were reacted with an anti-phospho-AMPK Thr172 antibody followed by an anti-rabbit IgG antibody after non-treatment and treatment with adenosine or AICAR. The nucleus was labeled with an anti-DAPI antibody. Fluorescent signals were detected with a laser scan confocal microscope (LSM 510; Zeiss, Welywyn Garden City, UK). The fluorescence intensity was quantified with an NIH Image software.

Western blotting
HuH-7 cells were lysed in a lysate solution [0.1% (v/v) Tween20, 0.1% (v/v) sodium dodecyl sulfate (SDS), 20 mM Tris-HCl, 150 mM NaCl, and 1% (v/v) protease inhibitor cocktail]. Lysates were centrifuged at 10,000 rpm for 10 min at 4°C, and the supernatant (30 μg protein) was loaded on 12% (v/v) SDS- polyacrylamide gel electrophoresis (SDS-PAGE), and separated proteins were transferred to polyvinylidene difluoride (PVDF) membranes. After blocking with TBST [150 mM NaCl, 0.1% (v/v) Tween20, and 20 mM Tris-HCl] containing 5% (v/v) bovine serum albumin, blotting membranes were reacted with an antibody against AMPKα1, AMPKα2, DIABLO, phosphoserine/threonine, or Bcl-X$_L$, followed by an HRP-conjugated anti-rabbit IgG antibody or anti-mouse IgG antibody. Immunoreactivity was detected with an ECL kit and visualized using a chemiluminescenece with an Image Gauge software (FUJIFILM, Tokyo, Japan).

Cell fractionation
HuH-7 cells were homogenized with a sonicator in a Buffer A solution (20 mM HEPES, 10 mM KCl, 1.5 mM MgCI$_2$, 1 mM EDTA, 1 mM EGTA, 1 mM dithiothreitol, 0.1 mM phenylmethyl-sulfonyl fluoride, and 250 mM sucrose, pH 7.5). Lysates were centrifuged at 1,000 x g for 10 min, and the supernatant was further centrifuged at 10,000 x g for 1 h. Then, the pellet resuspended in a Buffer A solution and the supernatant were used for the ensuing experiments as a mitochondrial and cytosolic fraction, respectively. Fractionation samples from a same amount of lysates were loaded on SDS-PAGE. It was confirmed that the mitochondrial components are reactive to an anti-prohibitin antibody, a mitochondrial marker, but that no immunoreactive signal is obtained with the cytosolic components.

Immunoprecipitation
HuH-7 cells were lysed in the lysate solution, and lysates (500 μg of protein) were incubated in the presence of an anti-phosphoserine/threonine antibody (1 μg) or an anti-Bcl-X$_L$ antibody (2 μg) overnight at 4°C. Then, 20 μl of protein G agarose was added to the lysates and incubated overnight at
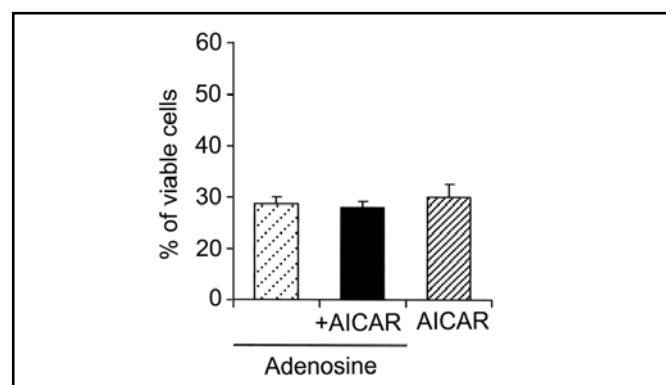

Fig. 1. AICAR induces HuH-7 cell death. HuH-7 cells were treated with adenosine alone (10 mM), AICAR (100 μM) alone, and adenosine (10 mM) together with AICAR (100 μM) for 48 h, and the cell viability was quantified with an MTT assay. In the graph, each column represents the mean (± SEM) percentage of basal levels (MTT intensities of cells untreated with adenosine) (n=4 independent experiments).

4°C. Extracts were dissolved in 40 μl of an SDS sample buffer [0.2 mM Tris-HCl, 0.04% (v/v) SDS, and 20% (v/v) glycerol, pH 6.8] followed by Western blotting.

Monitoring of in situ DIABLO mobilizations
DIABLO-GFP-pcDNA6/V5 together with and without the plasmid DNA for mutant Bcl-X$_L$ lacking Ser/Thr phosphorylation sites was transfected into HuH-7 cells. DIABLO mobilizations were monitored by detecting GFP signals at an excitation of 385 nm and an absorption of 510 nm, and mitochondrial localization was identified by detecting MitoTracker Red 580 at an absorption of 590 nm using a laser scanning microscopes (LSM510, Carl Zeiss Co., Ltd, Germany).
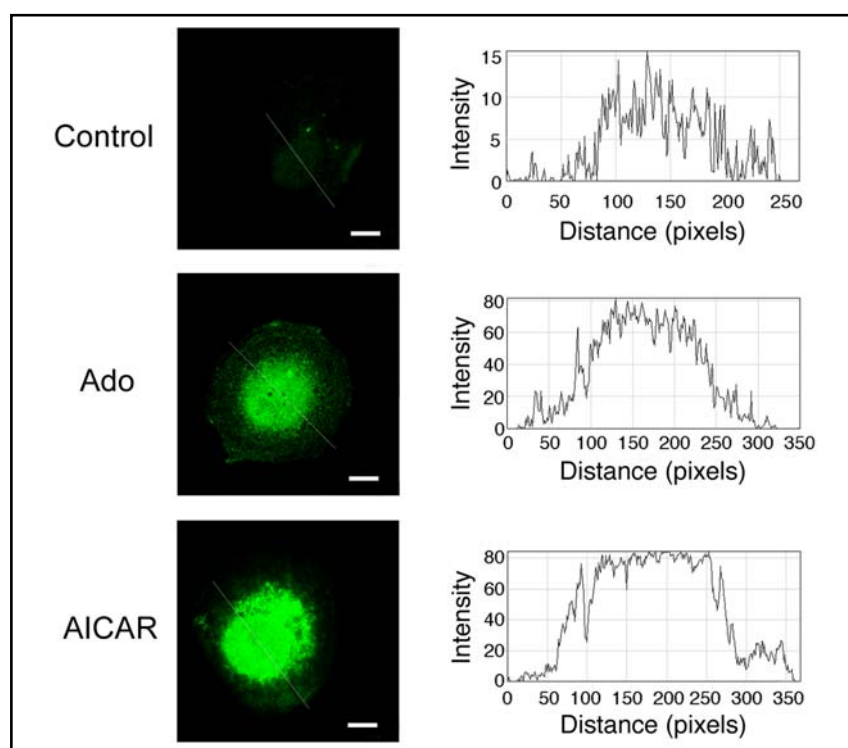
Enzymatic assay of caspase-3 activity
Caspase-3 activity was enzymatically assayed using a caspase-3 substrate peptide [1]. HuH-7 cells were lysed and reacted with the fluorescently labeled tetrapeptide at 37°C for 2 h. Fluorescent intensities were measured at an excitation of 400 nm and at an emission of 505 nm with a fluorometer (Fluorescence Spectrometer, F-4500, HITACHI, Tokyo, Japan).

Results

Extracellular adenosine activates AMPK in HuH-7 cells
Treatment with extracellular adenosine (10 mM) for 48 h decreased HuH-7 cell viability to approximately 37% of basal levels (Fig. 1). Notably, 5-aminoimidazole-4-carboxamide riboside (AICAR) (100 μM), an activator of AMPK [4], exhibited an effect similar to adenosine, but no synergistic reduction in the cell viability was obtained with co-treatment with adenosine and AICAR (Fig. 1). This suggests that adenosine induces HuH-7 cell apoptosis

Fig. 2. Extracellular adenosine activates AMPK. HuH-7 cells were reacted with an anti-phospho-AMPK Thr172 antibody before (Control) and after 6-h treatment with adenosine (Ado)(10 mM) or AICAR (100 µM). Scale bars, 10 µm. In the graphs, the fluorescent intensity was quantified with an NIH Image software. Note that a similar result was obtained with 4 independent experiments.

by a common mechanism shared with AICAR. If this is true, adenosine should activate AMPK. AMPK is activated by being phosphorylated at Thr172 [5, 6], and therefore, AMPK activation can be monitored by detecting AMPK phosphorylation at Thr172. In the immunocytochemistry using an anti-phospho-AMPK Thr172 antibody, AICAR (100 µM) markedly increased the phosphorylation intensity in HuH-7 cells as compared with control, and a similar increase was found with adenosine (10 mM) (Fig. 2). This confirms that adenosine activates AMPK in HuH-7 cells.

AMPK disrupts mitochondrial membrane potentials by phosphorylating Bcl-X$_L$

We next examined the effect of AMPK on mitochondrial membrane potentials using DePsipher™. DePsipher™, a mitochondrial activity marker, has the properties of aggregating upon membrane polarization forming an orange-red fluorescent compound. If the potential is disturbed, the dye has no access to the transmembrane space and remains in or reverts to its green monomeric form. For untreated cells, the mitochondria exhibited orange-red fluorescent signals at an absorbance of 590 nm (Fig. 3A) and no accumulation of green fluorescent signals at an absorbance of 530 nm (Fig. 3B). In contrast, 24-h treatment with adenosine (10 mM) accumulated green fluorescent signals (Fig. 3D) without orange-red fluorescent signals (Fig. 3C). Likewise, accumulation of green fluorescent signals alone was found
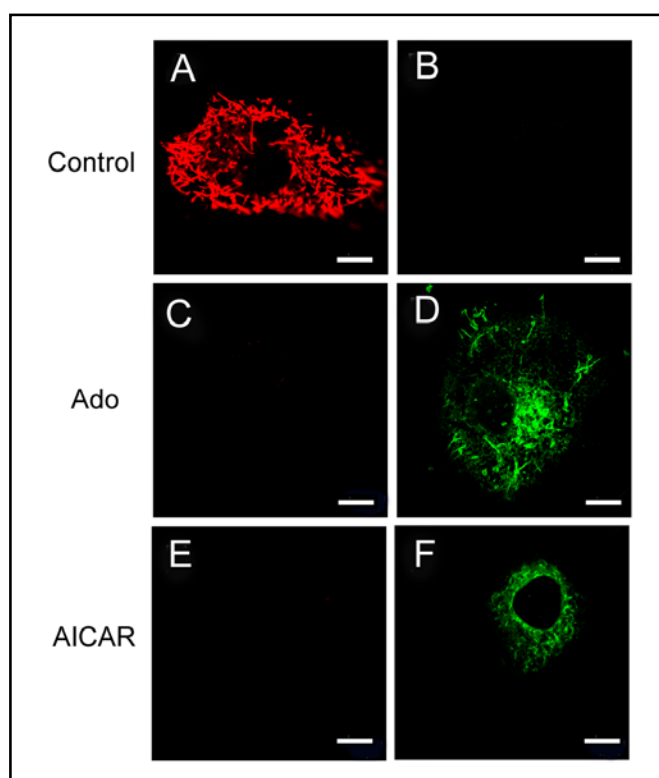

Fig. 3. AICAR disrupts mitochondrial membrane potentials. Mitochondrial membrane potentials were assayed using a DePsipher™ kit before (Control) and after 24-h treatment with adenosine (Ado)(10 mM) or AICAR (100 µM) in HuH-7 cells. Orange-red (A,C,E) and green fluorescent signals (B,D,F) were detected at an absorbance of 590 and 530 nm, respectively. Scale bars, 10 µm. Note that a similar result was obtained with 4 independent experiments.

Fig. 4. AMPK damages mitochondrial membrane potentials. (A) Western blotting was performed using an anti-AMPKα1 antibody and an anti-AMPKα2 antibody in HuH-7 cells 48 h after transfection with Mock (Control), the AMPKα1 siRNA, or the AMPKα2 siRNA. Mitochondrial membrane potentials were monitored after 24-h treatment with adenosine (Ado)(10 mM) or AICAR (100 μM) in cells expressing the AMPKα1 siRNA and/or the AMPKα2 siRNA (B) or dominant negative mutant AMPKα2 (D157A) (C). Scale bars, 10 μm. Note that a similar result was obtained with 4 independent experiments.
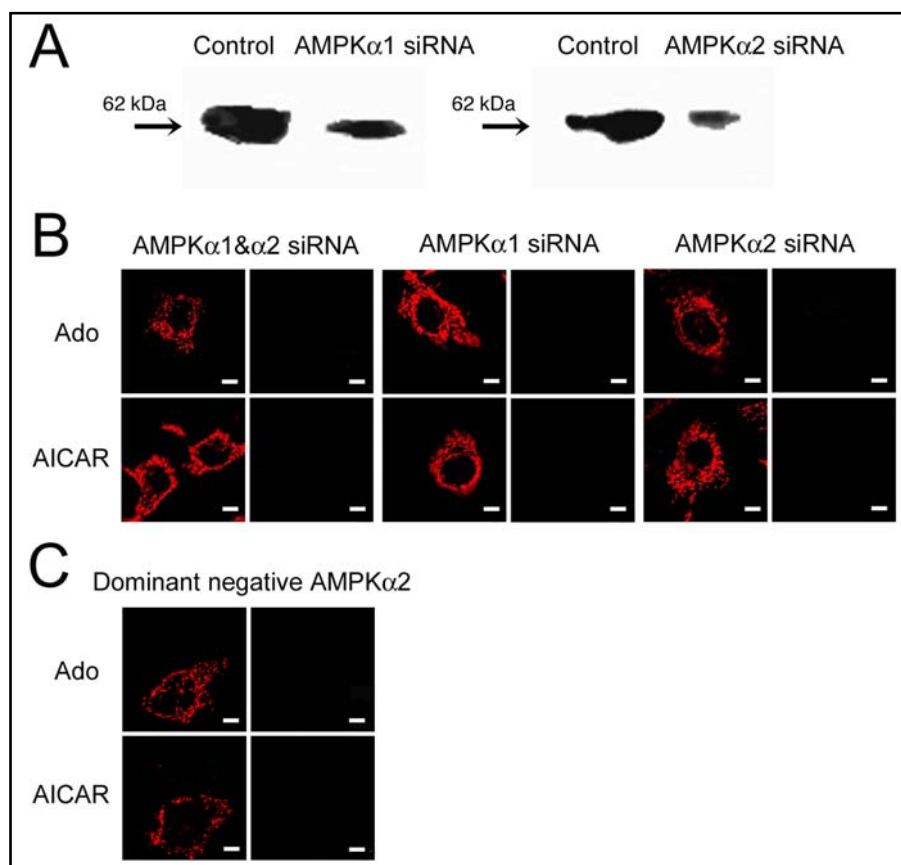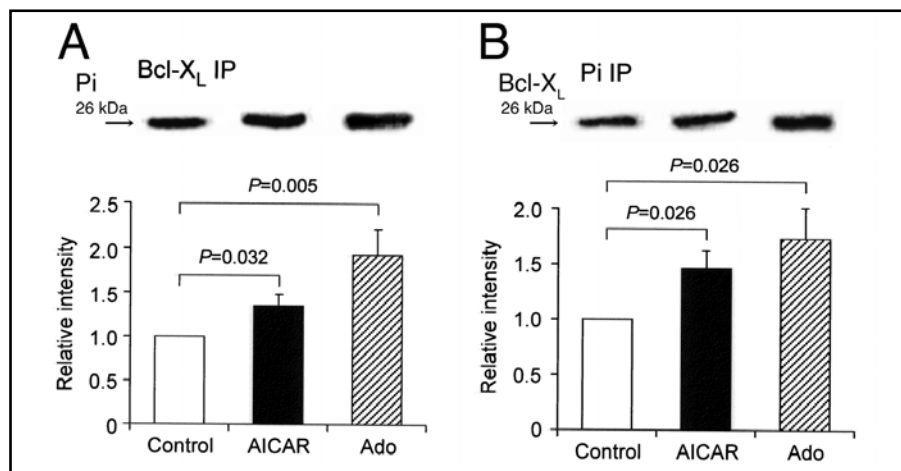

Fig. 5. AMPK phosphorylates Bcl-X$_L$. Lysates from HuH-7 cells were immuno-precipitated with an anti-Bcl-X$_L$ antibody (Bcl-X$_L$ IP) or an anti-phosphoserine/threonine antibody (Pi IP) followed by Western blotting with an anti-phosphoserine/threonine antibody (A) or an anti-Bcl-X$_L$ antibody (B), respectively. In the graphs, each column represents the mean (± SEM) ratio against control signal intensities (n=3-5 independent experiments). *P* values, unpaired *t*-test.

with AICAR (100 μM) (Fig. 3E,F), suggesting that AMPK, activated by adenosine, perturbs mitochondrial membrane potentials. To obtain further evidence for this, we constructed the siRNAs for AMPKα1 and AMPKα2 or the dominant negative mutant AMPKα2 (D157A) plasmid. A marked decrease in the expression of AMPKα1 and AMPKα2 protein was obtained by transfecting the AMPKα1 and AMPKα2 siRNA, respectively (Fig. 4A). For cells knocking-down both the AMPKα1 and AMPKα2 or each alone, adenosine (10 mM) or AICAR (100 μM) caused no accumulation of green fluorescent signals (Fig. 4B). Moreover, no accumulation of green fluorescent signals was found with cells expressing dominant negative mutant AMPKα2 (D157A) (Fig. 4C). These results account for AMPK-dependent disruption of mitochondrial membrane potentials in HuH-7 cells.

The Bcl-2 family such as Bcl-2 and Bcl-X$_L$ is recognized to protect the mitochondria from damaging. In the reverse transcription-polymerase chain reaction analysis, the Bcl-X$_L$ mRNA was expressed in HuH-7 cells, but the mRNAs for Bcl-2α and -2β were not detectable (data not shown). We, therefore, highlighted Bcl-X$_L$ as a target of AMPK. In the Western blot analysis, adenosine
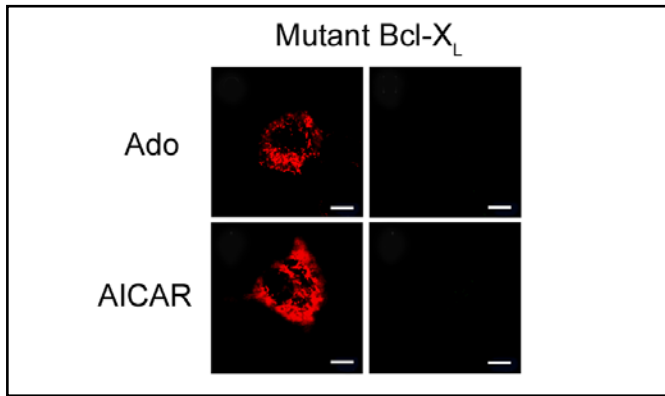
Fig. 6. AMPK damages mitochondrial membrane potentials by phosphorylating Bcl-X$_L$. Mitochondrial membrane potentials were monitored after 24-h treatment with adenosine (Ado)(10 mM) or AICAR (100 µM) in cells expressing mutant Bcl-X$_L$ lacking Ser/Thr phosphorylation sites. Scale bars, 10 µm. Note that a similar result was obtained with 4 independent experiments.
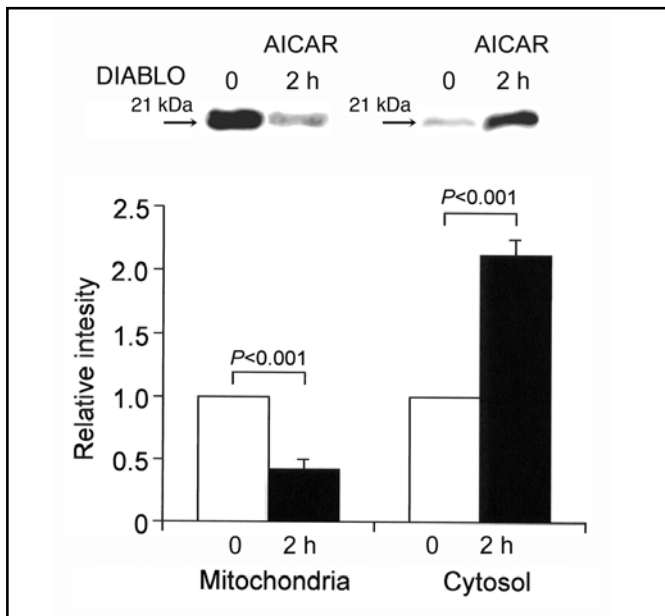

Fig. 7. AMPK increases cytosolic DIABLO but decreases mitochondrial DIABLO. Homogenates from HuH-7 cells untreated and treated with AICAR (100 µM) for 2 h were separated into the mitochondrial and cytosolic fraction, and Western blotting was carried out in each fraction using an anti-DIABLO antibody. In the graph, each column represents the mean (± SEM) ratio against basal signal intensities (0 h)(n=3 independent experiments). *P* values, unpaired *t*-test.

Fig. 8. AMPK stimulates DIABLO release from the mitochondria by phosphorylating Bcl-X$_L$. *In situ* DIABLO mobilizations were monitored by detecting GFP signals throughout 20 min after bath-application with AICAR (100 µM) in HuH-7 cells expressing DIABLO-GFP together without (Control)(A) and with mutant Bcl-X$_L$ lacking Ser/Thr phosphorylation sites (Mutant Bcl-X$_L$)(B). The mitochondria were identified with MitoTracker Red 580. Scale bars, 10 µm. Note that a similar result was obtained with 4 independent experiments.

(10 mM) or AICAR (100 µM) enhanced an immunoreactive signal against an anti-phosphoserine/threonine antibody for samples from HuH-7 cells immunoprecipitated with an anti-Bcl-X$_L$ antibody (Fig. 5A). Similarly, adenosine (10 mM) or AICAR (100 µM) enhanced an immunoreactive signal against an anti-Bcl-X$_L$ antibody for samples from HuH-7 cells
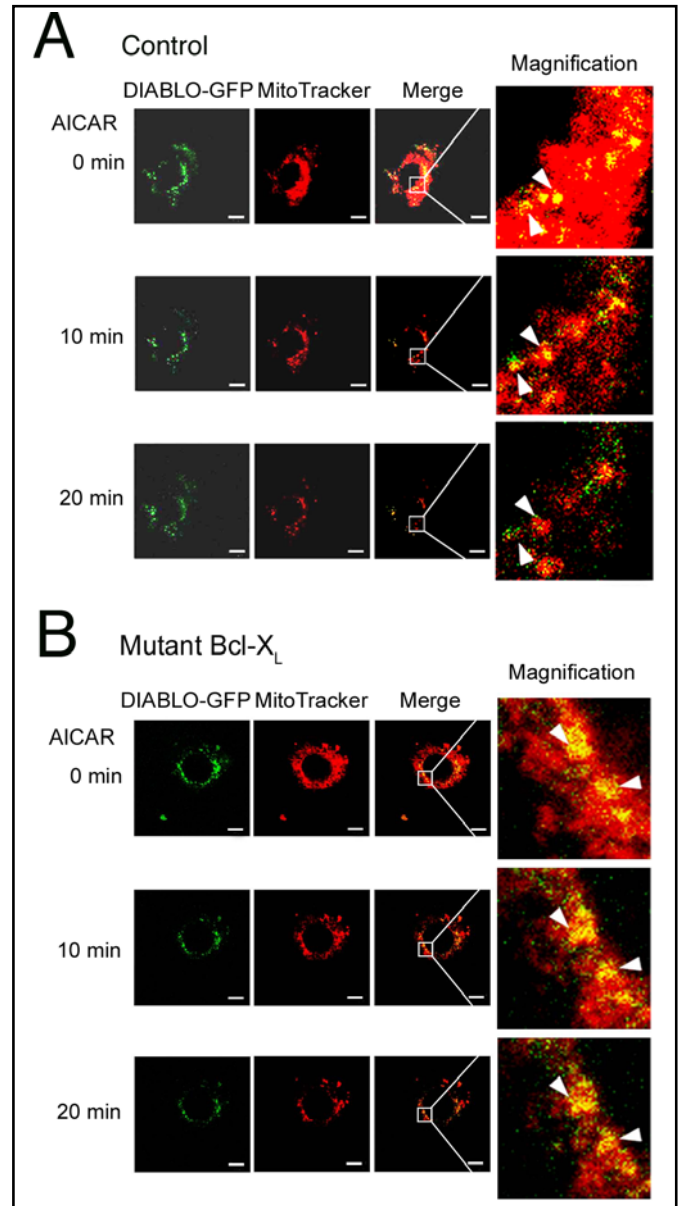
immunoprecipitated with an anti-phosphoserine/threonine antibody (Fig. 5B). It is indicated from these results that AMPK, activated by adenosine, phosphorylates Bcl-X$_L$. Notably, 24-h treatment with adenosine (10 mM) or AICAR (100 µM) never accumulated green fluorescent signals for HuH-7 cells expressing mutant Bcl-X$_L$ lacking Ser/Thr phosphorylation sites (Fig. 6). Collectively, these

results lead to a conclusion that AMPK perturbs mitochondrial membrane potentials by phosphorylating Bcl-X_L.

AMPK stimulates DIABLO release from the mitochondria and activates caspase-3

Mitochondrial damage could release a variety of mitochondrial proteins including DIABLO. In the Western blot analysis, 2-h treatment with AICAR (100 µM) decreased an immunoreactive signal against DIABLO in the mitochondrial fraction from HuH-7 cells, but conversely increased the signal in the cytosolic fraction (Fig. 7). This suggests that AMPK stimulates DIABLO release from the mitochondria. We further monitored *in situ* DIABLO mobilizations with a fluorescent imaging scan. AICAR (100 µM) attenuated DIABLO signals in the mitochondria, mostly bleaching at 20-min treatment (Fig. 8A), but the AICAR effect was otherwise prevented by expressing mutant Bcl-X_L lacking Ser/Thr phosphorylation sites (Fig. 8B). This implies that AMPK damages mitochondrial membrane potentials by phosphorylating Bcl-X_L, thereby stimulating DIABLO release from the mitochondria in HuH-7 cells.

In the enzymatic assay of caspase-3 activity, AICAR (100 µM) activated caspase-3, and the AICAR effect was abolished by expressing mutant Bcl-X_L lacking Ser/Thr phosphorylation sites (Fig. 9). This, in the light of the fact that DIABLO reduces activity of IAPs to inhibit caspase-3, -7, and -9 [7, 8], raises the possibility that AMPK activates caspase-3 by neutralizing caspase-3 inhibition due to IAP in response to DIABLO released from damaged mitochondria through Bcl-X_L phosphorylation (Fig. 10).

Discussion

Several avenues of evidence have pointed to AMPK as an inducer of apoptosis or proliferation in a variety of cancer cells. AICAR, an activator of AMPK, induces apoptosis of the rat hepatoma cell line FTO2B cells and inhibits growth of the human hepatoma cell line HepG2 cells [9]. AMPK is also shown to induce apoptosis in mouse astrocytoma but not normal brain cells [10]. As is the case with adenosine, AICAR induces GT3-TKB cell apoptosis [3]. Little, however, is known about the mechanism underlying AMPK-induced apoptotic cell death.

In the present study, extracellular adenosine or AICAR induced HuH-7 cell death, and no additional effect
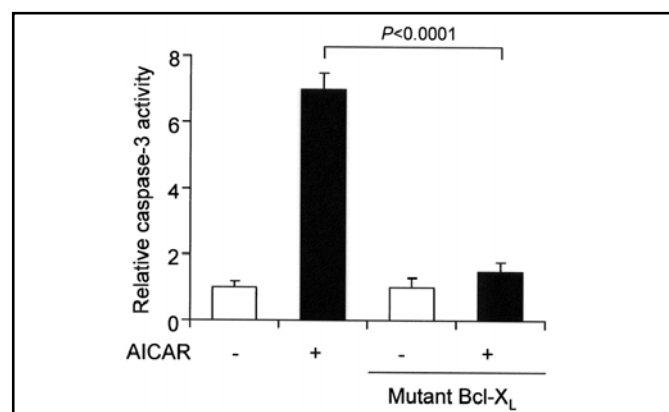

Fig. 9. AMPK activates caspase-3 by phosphorylating Bcl-X_L. After 24-h treatment with AICAR (100 µM), caspase-3 activity was assayed in HuH-7 cells non-expressing and expressing mutant Bcl-X_L lacking Ser/Thr phosphorylation sites (Mutant Bcl-X_L). In the graph, each column represents the mean (± SEM) ratio against basal caspase-3 activities (0 h)(n=4 independent experiments). *P* value, unpaired *t*-test.
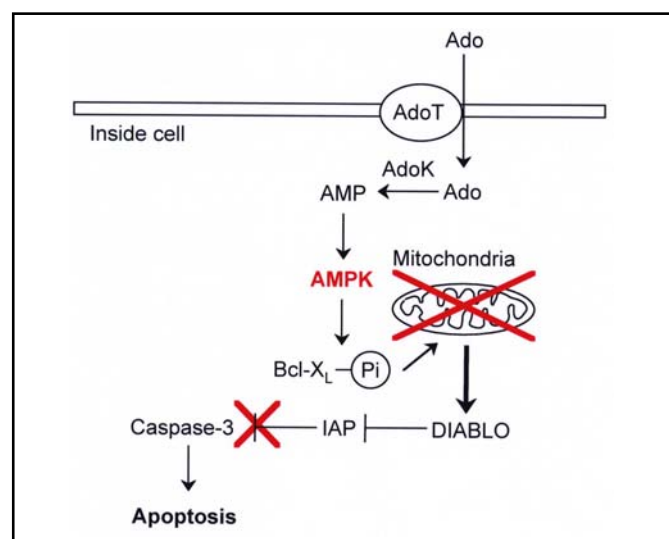

Fig. 10. Schematic diagram for an apoptotic pathway linked to adenosine/AMPK. Ado, adenosine; AdoT, adenosine transporter; AdoK, adenosine kinase; Pi, phosphorylation.

was obtained with co-treatment with adenosine and AICAR, suggesting the implication of AMPK in an adenosine-induced HuH-7 cell apoptosis. Adenosine actually activated AMPK in a fashion that mimics the AICAR effect. Adenosine or AICAR disrupted mitochondrial membrane potentials in HuH-7 cells, and the effect was inhibited by knocking-down AMPKα1 and/ or AMPKα2 or expressing dominant negative mutant AMPKα2 (D157A). This indicates that adenosine perturbs mitochondrial membrane potentials in an AMPK-dependent manner. The mitochondria express the Bcl family of proteins such as Bcl-2, Bcl-X_L, Bax, and Bad,

that promotes or prevents apoptosis [11-13]. Interestingly, adenosine or AICAR phosphorylated Bcl-X_L, and mitochondrial damage induced by adenosine or AICAR was prevented by expressing mutant Bcl-X_L lacking Ser/Thr phosphorylation sites. Taken together, adenosine appears to activate AMPK, to phosphorylate Bcl-X_L, causing disruption of mitochondrial membrane potentials in HuH-7 cells.

For a mitochondrial apoptotic pathway, oxidative stress-induced mitochondrial damage releases cytochrome c that forms an oligomeric complex with dATP or Apaf-1. The complex, in turn, activates caspase-9 followed by activation of the effector caspase-3, causing DNA degradation, i.e., apoptotic cell death [14-17]. A complicated finding in the present study was that in spite of mitochondrial damage adenosine induces HuH-7 cell apoptosis, independently of caspase-9 activation [1]. Mitochondrial damage triggers release of not only cytochrome c but other proteins such as DIABLO to inhibit IAP, an inhibitor of caspase-3, -7, and -9 [7, 8]. We have confirmed that adenosine increased presence of cytosolic DIABLO in concert with decreased mitochondrial DIABLO in HuH-7 cells [2]. In the present study, a similar effect was still obtained with AICAR. In the fluorescent assay of *in situ* DIABLO mobilizations in HuH-7 cells, AICAR attenuated DIABLO signals in the mitochondria, i.e., AICAR released DIABLO from the mitochondria, and the AICAR effect was inhibited by expressing mutant Bcl-X_L lacking Ser/Thr phosphorylation sites. AICAR activated caspase-3 in HuH-7 cells, and the activation was abolished by expressing mutant Bcl-X_L lacking Ser/Thr phosphorylation sites. Overall, these results indicate that AMPK, activated by adenosine, disrupts mitochondrial membrane potentials by phosphorylating Bcl-X_L, allowing DIABLO release from the mitochondria to activate caspase-3, possibly as a consequence from neutralizing caspase-3 inhibition due to IAP (Fig. 10). This may represent fresh insight into the pathway linked to AMPK for adenosine-induced HuH-7 cell apoptosis.

In conclusion, we show here that AMPK, activated by AMP that is converted from intracellularly transported adenosine, disrupts mitochondrial membrane potentials through Bcl-X_L phosphorylation, allowing DIABLO release from the mitochondria, thereby leading to caspase-3 activation, responsible for HuH-7 cell apoptosis.

References

1   Yang D, Yaguchi T, Yamamoto H, Nishizaki T: Intracellularly transported adenosine induces apoptosis in HuH-7 human hepatoma cells by downregulating c-FLIP expression causing caspase-3/-8 activation. Biochem Pharmacol 2007;73:1665-1675.
2   Yang D, Yaguchi T, Nakano T, Nishizaki T: Adenosine-induced caspase-3 activation by tuning Bcl-X_L/DIABLO/IAP expression in HuH-7 human hepatoma cells. Cell Biol Toxicol 2010;26:319-330.
3   Saitoh M, Nagai K, Nakagawa K, Yamamura T, Yamamoto S, Nishizaki T: Adenosine induces apoptosis in the human gastric cancer cells via an intrinsic pathway relevant to activation of AMP-activated protein kinase. Biochem Pharmacol 2004;67:2005-2011.
4   Bae EJ, Cho MJ, Kim SG: Metformin prevents an adaptive increase in GSH and induces apoptosis under the conditions of GSH deficiency in H4IIE cells. J Toxicol Environ Health A 2007;70:1371-1380.

5   Hardie DG, Carling D, Carlson M: The AMP-activated/SNF1 protein kinase subfamily: metabolic sensors of the eukaryotic cell? Annu Rev Biochem 1998;67:821-855.
6   Kemp BE, Mitchelhill KI, Stapleton D, Michell BJ, Chen ZP, Witters LA: Dealing with energy demand: the AMP-activated protein kinase. Trends Biochem Sci 1999;24:22-25.
7   Du C, Fang M, Li Y, Li L, Wang X: Smac, a mitochondrial protein that promotes cytochrome c-dependent caspase activation by eliminating IAP inhibition. Cell 2000;102:33-42.
8   Salvesen GS, Duckett CS: IAP proteins: blocking the road to death's door. Nat Rev Mol Cell Biol 2002;3:401-410.
9   Zhuge J: Overexpression of CYP2E1 induces HepG2 cells death by the AMP kinase activator 5'-aminoimidazole-4-carboxamide-1-b-D- ribofuranoside (AICAR). Cell Biol Toxicol 2009;25:253-263.
10   Mukherjee P, Mulrooney TJ, Marsh J, Blair D, Chiles TC, Seyfried TN: Differential effects of energy stress on AMPK phosphorylation and apoptosis in experimental brain tumor and normal brain. Mol Cancer 2008;7:37.

11   Cory S, Adams JM: The Bcl2 family: regulators of the cellular life-or-death switch. Nat Rev Cancer 2002;2:647-656.
12   Kroemer G: The proto-oncogene Bcl-2 and its role in regulating apoptosis. Nat Med 1997;3:614-620.
13   Wang X: The expanding role of mitochondria in apoptosis. Genes Dev 2001;15:2922-2933.
14   Green DR, Reed JC: Mitochondria and apoptosis. Science 1998;281:1309-1312.
15   Li LY, Luo X, Wang X: Endonuclease G is an apoptotic DNase when released from mitochondria. Nature 2001;412:95-99.
16   Loeffler M, Kroemer G: The mitochondrion in cell death control: certainties and incognita. Exp Cell Res 2000;256:19-26.
17   Susin SA, Lorenzo, HK, Zamzami N, Marzo I, Snow BE, Brothers GM, Mangion J, Jacotot E, Costantini P, Loeffler M, Larochette N, Goodlett DR, Aebersold R, Siderovski DP, Penninger JM, Kroemer G: Molecular characterization of mitochondrial apoptosis-inducing factor. Nature 1999;397:441-446.